Proceedings of the 4rd International Conference on Mechatronics and Smart Systems
DOI: 10.54254/2755-2721/2026.32474

Modeling and Error Compensation Method for Self-Heating Effect of DIC Camera Oriented to Intelligent Monitoring of Civil Structures

Ze Hui[1], Ruoqiang Feng[1*]

[1]School of Civil Engineering, Southeast University, Nanjing, China
**Corresponding Author. Email: hitfeng@163.com*

Abstract. Aiming at the problems of image point drift and degradation of measurement accuracy caused by the self-heating effect of cameras in the long-term intelligent monitoring of civil structures by Digital Image Correlation (DIC) technology, this paper designs special self-heating tests and internal parameter calibration tests under a constant temperature environment. The chip temperature is collected in real time through the camera SDK to quantitatively reveal the strong positive correlation between chip temperature and image point drift as well as core internal parameters. A self-heating noise regression model and an internal parameter-temperature mapping model are constructed, and an error compensation method without additional hardware investment is proposed. The test results show that the proposed method can reduce the image point drift error by more than 97%. After the correction of the two models, the errors are reduced to 0.0049~0.0054 Pixel and below 0.0064 Pixel respectively. This research can provide high-precision visual measurement technical support for the intelligent health monitoring of civil infrastructure such as bridges and transmission towers.

Keywords: Digital Image Correlation, Self-heating Effect of Camera, Intelligent Structural Health Monitoring, Intelligent Civil Engineering System

1. Introduction

Intelligent civil engineering is an important branch of intelligent systems, and Digital Image Correlation (DIC) technology has become a core method for the health monitoring of civil infrastructure [1,2]. In long-term monitoring, the image point drift and internal parameter distortion caused by the camera's self-heating effect can introduce a maximum measurement error of 0.25 Pixel, which directly restricts the reliability of intelligent monitoring systems [3,4]. Existing studies mostly focus on the laws of camera heat transfer and image deformation, lacking a systematic explanation of the mechanism of image point drift, and there are no quantifiable error correction models and engineering schemes adapted to civil engineering sites [5-8]. In response to this, this paper designs a special test for real-time collection of chip temperature, analyzes the correlation between temperature, image point drift and core internal parameters, constructs two types of self-heating error correction models, and proposes a compensation method without additional hardware.

DOI: 10.54254/2755-2721/2026.32474

The accuracy and reliability of the method are verified by tests, which provides technical support for the intelligent monitoring of civil structures.

2. Experimental design

2.1. Experimental principle

According to the rigid body motion theory, the theoretical displacement of an absolutely stationary speckle rigid plate is 0, and the displacement signal detected during the measurement process can be directly attributed to the image point drift error caused by camera self-heating, realizing accurate separation and quantification of the error. The core heat source of camera self-heating is the Joule heat generated by the operation of the image sensor. There is a significant deviation between the traditional temperature measurement on the camera body/lens surface and the actual chip temperature. Therefore, this study directly reads the chip temperature in real time by calling the thermal_get_temperature() function of the FLIR camera SDK, providing an accurate temperature reference for error traceability.

2.2. Experimental system and instruments

To eliminate environmental disturbances, the entire test system is placed in a closed constant temperature room to achieve constant control of temperature, humidity and illumination; the optical platform is integrated with precision damping vibration isolation pads to suppress external vibration interference; heat dissipation equipment such as computers is placed separately from the core components of photogrammetry to avoid the interference of heat dissipation on the camera temperature field. The layout of the test system is shown in Fig. 1, and the parameters of the core instruments are shown in Table 1.

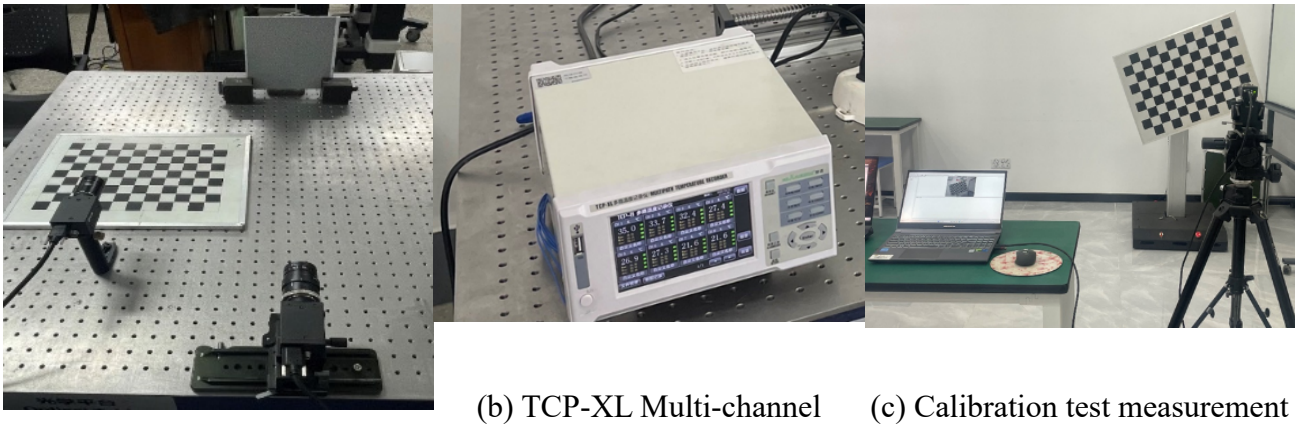

(a) Photogrammetry system

(b) TCP-XL Multi-channel Temperature Recorder

(c) Calibration test measurement system

Figure 1. Measurement system

Table 1. Models of instruments and equipment for self-heating test

Instruments and Equipment	Model Parameters
Industrial Camera	FLIR GS3-U3-41C6M-C, with a resolution of 2048×2048 and a pixel size of 5.5 μm×5.5 μm
Fixed-focus Lens	KOWA LM16HC

DOI: 10.54254/2755-2721/2026.32474

Table 1. (continued)

Optical Platform	Integrated with precision rubber damping vibration isolation pads and horizontal adjustment bearings
Calibration Specimen	200mm×200mm in size with a speckle size of 1mm; 12×9 checkerboard calibration board with a grid spacing of 60 mm
Temperature Recorder	TCP-XL Multi-channel Temperature Recorder
Automatic Calibration Vehicle	Including chassis, lifting/rotating/pitching mechanisms, with Bluetooth remote control for the pose transformation of the calibration board

2.3. Experimental procedure

Before the test, the temperature of the constant temperature room is stabilized at 22 ℃ (for self-heating test) or 17.5 ℃ (for calibration test), both within the suitable range for high-precision photogrammetry. The perpendicularity error between the camera optical axis and the specimen plane is adjusted to be ≤0.1°. The aperture is set to f/8, the exposure time to 6 ms, and the acquisition frame rate to 5 fps (for self-heating test) or 4 fps (for calibration test) to ensure that the speckles/corner points of the calibration board are imaged clearly without distortion.

Start the camera, temperature recorder and data acquisition software synchronously for continuous acquisition for 90 minutes: in the self-heating test, 1 image is saved every 10 frames, and the chip temperature, image point drift error and ambient temperature are recorded synchronously; in the calibration test, images are saved every frame at the initial stage, and 1 image is saved every 8 frames after the temperature rises to 28℃. During the test, the camera chip temperature is exported in real time through the improved 2D-DIC software, the image point drift errors $E_x$and E_y are obtained by solving the image displacement with the traditional 2D-DIC software, and the camera internal parameters Fx, Fy, u_0, v_0 are solved synchronously by the internal parameter calibration algorithm. The indoor ambient temperature is recorded synchronously by the TCP-XL Multi-channel Temperature Recorder at an interval of 2 seconds, and the time axis deviation of each device's data is controlled within ±0.1 second to ensure the spatiotemporal matching of temperature and error data. After the measurement, the camera is turned off and left to stand for 2 hours until the chip temperature returns to the initial value. All parameters remain unchanged, and the test is repeated 3 times to reduce random errors.

3. Analysis of self-heating effect and image point drift error

3.1. Correlation between temperature and image point drift

The indoor temperature remains stable throughout the test, eliminating environmental interference. The camera chip temperature rises from the initial 19.95 ℃ to 34.05 ℃, and the heating process shows an obvious phased characteristic: the heating rate is fast in the first 45 minutes and basically stable after reaching the peak; the variation law of the image point drift error is highly synchronous with the chip temperature. The X-axis error increases from 0 Pixel to 0.210 Pixel, rising rapidly in the first 60 minutes, and the Y-axis error increases from 0 Pixel to 0.258 Pixel, rising rapidly in the first 45 minutes, both tending to be stable after the temperature is constant.

Pearson correlation analysis is used to quantitatively verify the correlation, and the results are shown in Table 2. The data of the three tests are in good consistency. The correlation coefficients between the X-axis and Y-axis image point drift errors and the chip temperature reach 0.905~0.906

DOI: 10.54254/2755-2721/2026.32474

and 0.940 respectively, with a two-tailed significance P<0.001, confirming an extremely strong positive correlation between them. The increase of chip temperature is the core inducement of image point drift.

Table 2. Correlation analysis between image point drift measurement error and camera chip temperature change

FLIR GS3-U3-41C6M-C With KOWA LM16HC		Horizontal Image Point Drift Error		Vertical Image Point Drift Error	
		Pearson Correlation	Sig (2-tailed)	Pearson Correlation	Sig (2-tailed)
Temperature	Self-heating Test 1	0.906	< 0.001	0.940	< 0.001
	Self-heating Test 2	0.905	< 0.001	0.940	< 0.001
	Self-heating Test 3	0.905	< 0.001	0.940	< 0.001

3.2. Establishment of self-heating noise regression model

Based on the data of Test 1, the least square method is used to construct a linear regression model between the chip temperature T and the image point drift error, in the form of Eqs. (1)-(2). The model parameters and verification indicators are shown in Table 3. The goodness of fit of the models all exceeds 0.8, with a significance P<0.001 and no multicollinearity (VIF=1), showing an excellent fitting effect.

$$E_x = 0.021 \times T - 0.543 \tag{1}$$

$$E_y = 0.028 \times T - 0.730 \tag{2}$$

where: E_x is the X-axis image point drift error (Pixel); E_y is the Y-axis image point drift error (Pixel); T is the camera chip temperature (℃).

Table 3. Regression analysis between image point drift measurement error and camera chip temperature change

FLIR GS3-U3-41C6M-C With KOWA LM16HC	Horizontal Image Point Drift Error					Vertical Image Point Drift Error				
	Slope a	Intercep b	Goodness of Fit R^2	Significance	VIF	Slope a	Intercep b	Goodness of Fit R^2	Significance	VIF
Temperature	0.021	-0.543	0.820	<0.001	1	0.028	-0.730	0.884	<0.001	1

Verified by Tests 2 and 3, the Mean Squared Error (MSE) of the model prediction is as low as 0.00049~0.00052 and 0.00049~0.00061 respectively. After correction, the average image point drift error is reduced from 0.198~0.231 Pixel to 0.0049~0.0054 Pixel, with an error reduction rate of about 97.5%, indicating extremely high prediction accuracy and reliability. The prediction results are shown in Fig. 2.

DOI: 10.54254/2755-2721/2026.32474

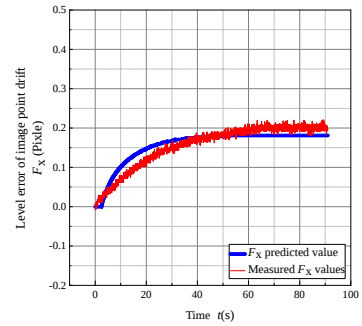

(a) Horizontal image point drift error of Test 2

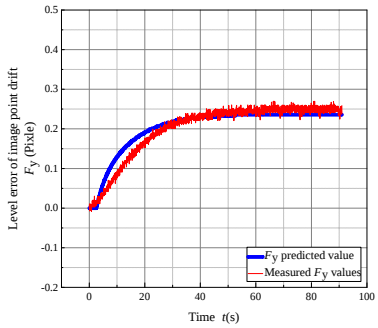

(b) Vertical image point drift error of Test 2

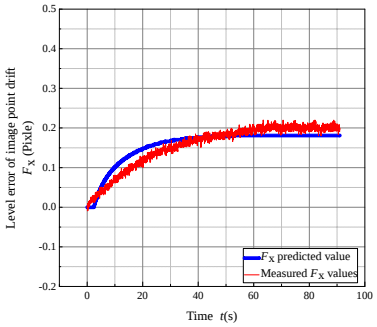

(c) Horizontal image point drift error of Test 3

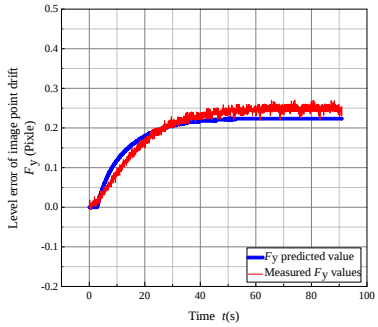

(d) Vertical image point drift error of Test 3

Figure 2. Comparison between predicted values of regression model and measured values of tests

4. Temperature mapping model of camera internal parameters

The increase of chip temperature caused by camera self-heating leads to the thermal expansion of internal optical components, changing the core internal parameters of the camera, which is the core inducement of image point drift error. Calibration tests show that when the chip temperature rises from 17.70℃ to 33.05℃, the variation ranges of the X/Y-axis focal lengths Fx/Fy and the principal point coordinates u_0/v_0 are significant and show an obvious upward trend with the increase of temperature; the variation range of the radial/tangential distortion coefficients is extremely small (≤3%), having no significant impact on the measurement accuracy.

The results of Pearson correlation analysis are shown in Table 4. The correlation coefficients between Fx, Fy, u_0, v_0 and the chip temperature reach 0.977~0.979, with a two-tailed significance P<0.001, confirming an extremely strong positive correlation between the core internal parameters and the chip temperature.

Table 4. Correlation analysis between camera internal parameters and camera chip temperature change

FLIR GS3-U3-41C6M-C With KOWA LM16HC		Focal Length Fx		Focal Length Fy		Principal Point u_0		Principal Point v_0	
		Pearson Correlation	Sig (2-tailed)	Pearson Correlation	Sig (2-tailed)	Pearson Correlation	Sig (2-tailed)	Pearson Correlation	Sig (2-tailed)
Temperature	Calibration Test 1	0.978	<0.001	0.979	<0.001	0.978	<0.001	0.979	<0.001
	Calibration Test 2	0.977	<0.001	0.977	<0.001	0.978	<0.001	0.979	<0.001

DOI: 10.54254/2755-2721/2026.32474

Calibration Test 3	0.978	<0.001	0.978	<0.001	0.979	<0.001	0.978	<0.001

Based on the data of Test 1, the least square method is used to construct a linear mapping model between the core internal parameters and the chip temperature, in the form of Eqs. (3)-(6). The model parameters and verification indicators are shown in Table 5. The goodness of fit of the models all exceeds 0.95, with a significance P<0.001 and no multicollinearity, showing an excellent fitting effect.

Table 5. Regression analysis results between camera internal parameters and chip temperature

Internal Parameter / Pixel	FLIR GS3-U3-41C6M-C With KOWA LM16HC						
	Slope a	Intercep b	Goodness of Fit R^2	Significance	VIF	Regression Equation	
Fx	0.166	2985.923	0.957	<0.001	1	$F_x = 0.166 \times T + 2985.923$	(3)
Fy	0.129	2986.905	0.958	<0.001	1	$F_y = 0.129 \times T + 2986.905$	(4)
u_0	0.191	1011.837	0.957	<0.001	1	$u_0 = 0.191 \times T + 1011.837$	(5)
v_0	0.197	1012.925	0.958	<0.001	1	$v_0 = 0.197 \times T + 1012.925$	(6)

where: Fx and Fy are the X and Y axis focal lengths of the camera (Pixel); u_0 and v_0 are the principal point coordinates of the camera (Pixel); T is the camera chip temperature (℃).

Verified by Test 2, the Mean Squared Error (MSE) of the model prediction is as low as 0.0104~0.0159. When applied to the correction of image sequences, the average image point drift error is reduced to below 0.0064 Pixel, with an error reduction rate of about 97.2%, which can eliminate the measurement error caused by the self-heating effect from the physical origin of imaging. The comparison between the predicted values of the regression model and the measured values of the test is shown in Fig. 3.

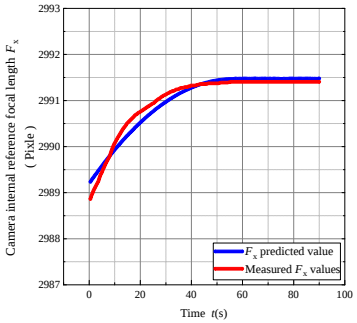

(a) X-axis focal length Fx

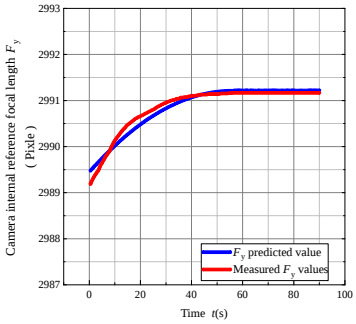

(b) Y-axis focal length Fy

DOI: 10.54254/2755-2721/2026.32474

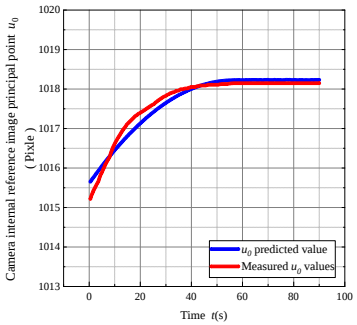

(c) Principal point u_0

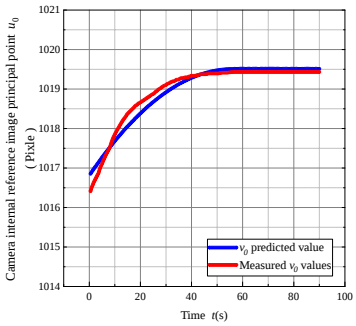

(d) Principal point v_0

Figure 3. Curves of camera core internal parameters changing with temperature

5. Establishment of self-heating noise regression model

Based on the self-heating noise regression model and internal parameter-temperature mapping model constructed in this paper, combined with the core application scenarios of DIC measurement for civil structures, this paper proposes two self-heating error compensation methods realized by pure software algorithms without additional hardware investment, which can be directly integrated into the existing DIC measurement systems and provide a feasible error suppression scheme for the intelligent monitoring of civil structures. The design of both methods is based on the core law verified by the tests in this paper: the camera chip temperature has a strong linear positive correlation with the image point drift error and core internal parameters, which can be accurately predicted by linear models without hardware modification of the existing monitoring system.

5.1. Direct compensation method

This method is adapted to the on-site long-term health monitoring scenarios of civil infrastructure such as bridges, transmission towers and long-span spatial structures. Such scenarios have strict requirements on the system modification amount and edge-side computing power, and the core demand is to eliminate the systematic error accumulated by self-heating and ensure the accuracy of structural deformation trend monitoring.

Core principle of the method: Taking the chip temperature read in real time by the camera SDK as the only input, substitute it into the self-heating noise regression model Eqs. (1)-(2) constructed in this paper to accurately predict the X/Y-axis image point drift systematic error at the current temperature, and directly deduct the error from the measured displacement results solved by DIC to obtain the real structural deformation data. This method does not need to modify the original image and the core solution process of DIC, and only performs post-processing on the displacement results, with low implementation difficulty and low computing power demand.

$$E_x = 0.021 \times T - 0.543 \tag{1}$$

$$E_y = 0.028 \times T - 0.730 \tag{2}$$

DOI: 10.54254/2755-2721/2026.32474

where: E_x is the X-axis image point drift error (Pixel); E_y is the Y-axis image point drift error (Pixel); T is the camera chip temperature (℃).

Core operation process: ① Before the formal monitoring, complete the pre-test under the on-site working conditions and calibrate the regression model parameters corresponding to the imaging parameters; ② Collect images and chip temperature synchronously during the monitoring to ensure that their time axis deviation is ≤±0.1s; ③ Substitute into the model to calculate the real-time drift error, and deduct the error from the DIC displacement results to obtain the real deformation data.

Verified by 3 repeated tests in this paper, this method can reduce the average image point drift error from 0.198~0.231 Pixel to 0.0049~0.0054 Pixel, with an error reduction rate of 97.5%, which fully meets the accuracy requirements of on-site long-term monitoring.

5.2. Root cause compensation method

This method is adapted to the high-precision measurement scenarios in the laboratory such as mechanical property tests of civil engineering materials and static/fatigue tests of structural components. Such scenarios have extremely high requirements on the full-field deformation measurement accuracy and need to eliminate the systematic error from the physical origin of imaging.

Core principle of the method: Based on the internal parameter-temperature mapping model (Eqs. 3-6) constructed in this paper, take the real-time chip temperature as the input to calculate the core internal parameters of the camera at the current temperature, construct a corrected internal parameter matrix, complete the thermal distortion correction of each frame of image before carrying out DIC solution, and eliminate the self-heating error from the physical origin of imaging.

$$F_x = 0.166 \times T + 2985.923 \tag{3}$$

$$F_y = 0.129 \times T + 2986.905 \tag{4}$$

$$u_0 = 0.191 \times T + 1011.837 \tag{5}$$

$$v_0 = 0.197 \times T + 1012.925 \tag{6}$$

where: F_x and F_y are the X and Y axis focal lengths of the camera (Pixel); u_0 and v_0 are the principal point coordinates of the camera (Pixel); T is the camera chip temperature (℃).

Core operation process: ① Complete pre-calibration before the test to obtain the internal parameter-temperature mapping model corresponding to the working conditions; ② Collect image sequences and chip temperature synchronously during the test; ③ Calculate the real-time internal parameters for each frame of image and complete the thermal distortion correction of the image; ④ Carry out DIC solution based on the corrected image to obtain high-precision full-field deformation results.

Verified by the tests in this paper, this method can reduce the average image point drift error to below 0.0064 Pixel, with an error reduction rate of 97.2%, which can meet the requirements of high-

DOI: 10.54254/2755-2721/2026.32474

precision laboratory tests.

5.3. Suggestions on method selection

For the on-site long-term, low computing power and large field of view intelligent monitoring of civil structures, the direct compensation method is preferred to achieve effective error suppression with the minimum transformation cost; for the material and component performance tests with small field of view, high precision and short cycle in the laboratory, the root cause compensation method is preferred to achieve the highest precision full-field deformation measurement. For extreme working conditions beyond the test temperature range of this paper (17.7℃~34.05℃), the model parameters need to be recalibrated through pre-tests, and the root cause compensation method is preferred to ensure the accuracy.

6. Conclusions and prospects

Aiming at the problem of accuracy degradation caused by the camera self-heating effect of 2D-DIC technology in the intelligent monitoring of civil structures, this paper draws the following core conclusions through special tests, law analysis and model construction:

(1) The camera chip temperature is the core inducement of image point drift error, and there is a statistically reliable strong positive correlation between them (the maximum Pearson correlation coefficient is 0.940, $P<0.001$). Under the test conditions, when the chip temperature rises from 19.95 ℃ to 34.05 ℃, the maximum drift errors of the X/Y axis reach 0.210/0.258 Pixel, and the errors show synchronous phased characteristics with temperature changes.

(2) The maximum goodness of fit of the constructed self-heating noise regression model is 0.884 ($P<0.001$). Verified by 3 repeated tests, the corrected image point drift error is reduced from 0.198~0.231 Pixel to 0.0049~0.0054 Pixel, with an error reduction rate of 97.5%, realizing high-precision prediction and correction of drift error.

(3) The camera core internal parameters (F_x, F_y, u_0, v_0) have an extremely strong linear positive correlation with the chip temperature (the maximum Pearson correlation coefficient is 0.979, $P<0.001$), and the influence of distortion coefficients can be ignored; the goodness of fit of the internal parameter-temperature mapping model is ≥0.957, with an error reduction rate of 97.2% after correction, which suppresses the self-heating error from the physical origin of imaging.

(4) The direct compensation method and root cause compensation method are proposed, which can realize error correction only through software algorithms without additional hardware, adapted to the on-site long-term monitoring of civil structures and high-precision laboratory test scenarios respectively, and can be directly integrated into the existing DIC systems with remarkable engineering practicability.

In the future, the test coverage of cameras with multiple models and parameters will be expanded to construct a generalized self-heating error correction model and reduce the engineering pre-calibration cost; combined with the special needs of smart grid and intelligent transportation in conferences, verification under complex field working conditions will be carried out to realize seamless integration with the civil intelligent monitoring system; the error coupling laws under complex working conditions such as dynamic measurement and environmental temperature change will be explored to improve the long-term stability and applicability of the model in the whole-life cycle monitoring of infrastructure.

DOI: 10.54254/2755-2721/2026.32474

References

[1] Pan B, Yu L, Wu D. High-Accuracy 2D Digital Image Correlation Measurements with Bilateral Telecentric Lenses: Error Analysis and Experimental Verification. Experimental Mechanics. 2013; 53: 1719-1733.
[2] Tian L, Zhao J, Pan B, Wang Z. Full-Field Bridge Deflection Monitoring with Off-Axis Digital Image Correlation. Sensors. 2021; 21: 5058.
[3] Daakir M, Zhou Y, Deseilligny MP, Thom C, Martin O, Rupnik E. Improvement of photogrammetric accuracy by modeling and correcting the thermal effect on camera calibration. ISPRS Journal of Photogrammetry and Remote Sensing. 2019; 148: 142-155.
[4] Yu L, Lubineau G. Modeling of systematic errors in stereo-digital image correlation due to camera self-heating. Scientific Reports. 2019; 9.
[5] Ma S, Zhou S, Ma Q. Image distortion of working digital camera induced by environmental temperature and camera self-heating. Optics & Lasers in Engineering. 2019.
[6] Zhou S, Zhu H, Ma Q, Ma S. Heat Transfer and Temperature Characteristics of a Working Digital Camera. Sensors. 2020; 20: 2561.
[7] Feng D, Feng MQ. Vision-based multipoint displacement measurement for structural health monitoring. Structural Control and Health Monitoring. 2016; 23: 876-890.
[8] Pan B, Tian L, Song X. Real-time, non-contact and targetless measurement of vertical deflection of bridges using off-axis digital image correlation. NDT & E International. 2016; 79: 73-80.